

Flow sensitivity and coherence in steady-state free spin precession

Rodrigo Bagueira de Vasconcellos Azeredo,¹ M. Engelsberg,² and Luiz A. Colnago³

¹*Instituto de Química de São Carlos, Universidade de São Paulo, Avenida Dr. Carlos Botelho 1465, 13560-970 São Carlos, São Paulo, Brazil*

²*Departamento de Física, Universidade Federal de Pernambuco, Cidade Universitária, 50670-901, Recife, Pernambuco, Brazil*

³*Embrapa Instrumentação Agropecuária, Rua XV de Novembro 1452, 13560-970, São Carlos, São Paulo, Brazil*

(Received 8 February 2001; published 18 June 2001)

Steady-state free precession (SSFP) of nuclear spins in the presence of a magnetic field gradient is known to be very sensitive to flow. We present a theoretical and experimental study of flow sensitivity in a regime where the spacing of the radio-frequency pulses is extremely short compared with the free induction decay time and the relaxation times. Under these rather drastic conditions, a truly continuous wave free precession (CWFP) regime is established, in which, unlike standard SSFP, a large degree of coherence is preserved. This leads to a quite different flow sensitivity, which is significant even when very small magnetic field gradients are present. The unspoiled coherence is predicted to cause different flow effects which we confirmed experimentally. Tailored flow sensitivity can be achieved by adjusting the frequency offset from resonance, which plays a dominant role in the CWFP regime.

DOI: 10.1103/PhysRevE.64.0163XX

PACS number(s): 47.62.+q, 47.60.+i, 47.15.-x, 87.61.Lh

I. INTRODUCTION

Nuclear magnetic resonance (NMR) is a powerful tool for studying bulk flow and diffusion [1,2]. One of its main goals is to monitor fluid transport, either on a microscopic scale [3–6] or macroscopically when external gradients of concentration or pressure are present [7–12]. In particular, steady-state free precession (SSFP) [13–16] has been shown to be very effective in the specific case of medical imaging [17–20]. In its simplest version, a train of equally spaced radio-frequency (rf) pulses with period T_p is applied to a system of spins in a liquid near the resonant frequency $\gamma B_0/2\pi$. Here $B_0\mathbf{k}$ denotes the external static magnetic field and γ the magnetogyric ratio of the nuclei. If T_p is shorter than or at most of the same order as the transverse relaxation time T_2 , two types of steady-state signal, generally of different amplitudes, can be observed before and after each rf pulse. In the absence of bulk flow and neglecting diffusion, the amplitudes of these two signals can be predicted from Bloch's equations by considering the evolution of independent isochromats. Analytical expressions for the SSFP magnetization components have been obtained [15,16] and shown to depend upon the transverse (T_2) and longitudinal (T_1) relaxation times, the tip angle α of the rf pulses, the frequency offset from resonance (ϖ_0), and T_p .

One of the most striking characteristics of SSFP is its sensitivity to flow in the presence of an applied magnetic field gradient G along the direction of motion. Unfortunately, the problem becomes difficult to treat analytically and has been approached numerically using Monte Carlo (MC) and other techniques [18,19]. For a given isochromat with velocity v , the precession angle during the time interval T_p is no longer constant but rather increases by the amount $\phi = \gamma G v T_p^2$ in each new interval [18,19]. As a consequence translational time invariance is lost and a steady state, of the simple type prevailing in the absence of flow, no longer exists. Numerical simulations of the time evolution of a large number of isochromats have shown, however, that for uni-

formly distributed phases the ensemble average transverse magnetization does reach such a steady state, as observed experimentally [19].

An approximate partition analysis which treats the flow and diffusion sensitivity of SSFP in a way that permits better insight into the problem than MC calculations has been proposed by Gudbjartsson and Patz [18]. It has been shown to yield excellent results for ratios T_2/T_p as large as 2 but becomes less accurate for larger values of this ratio. In contrast, the continuous wave free precession (CWFP) regime is characterized by values of T_2/T_p that can be as large as 10^4 , thus requiring a different approach.

We here treat the problem of flow sensitivity in the CWFP regime numerically, using a direct matrix iteration algorithm. For realistic CWFP parameters, the effect of diffusion is expected to be negligible and it is not included in the algorithm in its present version. We show that, even though averaging over a uniform distribution of isochromat phases is by no means permissible in CWFP, a special steady state can nevertheless be established. The largely unspoiled coherence in the CWFP regime leads to a flow sensitivity that exhibits peculiar interference effects governed by the frequency offset from resonance. Experimental data that confirm the theoretical predictions are presented.

II. FLOW SENSITIVITY IN CWFP

Consider a train of rf pulses of frequency $\omega/2\pi$ which can be considered as pure rotations of angle α about the x axis of a reference frame that rotates with angular frequency ω . Let ϖ_0 be the average precession frequency of a group of isochromats in this rotating frame and denote the width of the distribution of precession frequencies by $1/T_2^*$. For an isochromat with frequency ϖ_0 , the precession angle in each period, given by $\psi = \varpi_0 T_p$, is constant in the absence of flow. Moreover, the establishment of a CWFP regime requires that the spread in precession angles $\Delta\psi = \Delta\varpi_0 T_p = T_p/T_2^*$ be very small. For our experiments, we chose T_p

≈ 0.3 msec with a free induction decay time constant $T_2^* \approx 20$ msec, permitting us to satisfy this condition quite comfortably. Magnetic field gradients must consequently also be kept quite small. For a cylindrical sample of length $l=0.4$ cm and radius $a=0.4$ cm, typical values of magnetic field gradient strengths along the cylindrical axis were $G \approx 0.09$ G/cm.

In the absence of flow, the steady-state components of magnetization in the rotating frame for an isochromat precessing with angular frequency ϖ_0 and advancing a constant angle $\psi = \varpi_0 T_p$ in each period are given by [15]

$$(M_x^-)_s = (1 - E_1)E_2(\sin \alpha)(\sin \psi) \frac{1}{D(\psi)}, \quad (1)$$

$$(M_y^-)_s = (1 - E_1)[E_2(\sin \alpha)(\cos \psi) - E_2^2(\sin \alpha)] \frac{1}{D(\psi)}, \quad (2)$$

$$(M_z^-)_s = (1 - E_1)[1 - E_2(\cos \psi) - E_2(\cos \alpha) \times (\cos \psi - E_2)] \frac{1}{D(\psi)}, \quad (3)$$

with

$$D(\psi) = [1 - E_1(\cos \alpha)][1 - E_2(\cos \psi) - [E_2 - \cos \psi][E_1 - \cos \alpha]E_2]. \quad (4)$$

$(M_\mu^-)_s$ ($\mu = x, y, z$) in Eqs. (1)–(3) refer to magnetization components immediately preceding a rf pulse, which are related to an echo signal. Moreover, the magnetization components $(M_\mu^+)_s$ immediately following a rf pulse, related to a free induction decay (FID), can be obtained by a rotation of angle α about the x axis. These components are normalized relative to the thermal equilibrium value and the relaxation factors that appear in Eqs. (1)–(4) are defined as $E_1 = \exp(-T_p/T_1)$ and $E_2 = \exp(-T_p/T_2)$.

The amplitude of the transverse magnetization $|M_{xy}| = (M_x^2 + M_y^2)^{1/2}$, as well as its phase, can be calculated from Eqs. (1)–(4) and completely describe the observed signals. The conditions $T_p \ll T_2^* \ll T_2$ and consequently $T_p \ll T_1$, which prevail in the CWFP regime, can be seen by inspection of Eqs. (1)–(4) to yield FID and echo signals of equal amplitudes. Furthermore, since the decay time of these signals is much longer than T_p , a continuous wave signal of amplitude $|M_{xy}^-|_s = |M_{xy}^+|_s$ is obtained [21]. For the chosen values of T_p and T_2^* , the dispersion of offset angles $\Delta\psi$ was sufficiently small to make unnecessary an integration over the angle ψ . This was confirmed by the good agreement between the predictions of Eqs. (1)–(4) and our measurements of signal amplitude as a function of ψ in the absence of flow.

We next consider quantitatively the problem of flow sensitivity. Since the precession angle in the rotating frame no longer remains constant but rather advances an additional angle $\phi = \gamma G v T_p^2$ in each new cycle, the echo magnetization components $(\mathbf{M}^-)_{n+1}$ at interval $n+1$ can be related to those at interval n by the matrix equation

$$(\mathbf{M}^-)_{n+1} = R(n, \phi, \psi)(\mathbf{M}^-)_n + (1 - E_1)\mathbf{M}_{\text{eq}}, \quad (5)$$

where $R(n, \phi, \psi)$ includes rotation about the x axis by angle α , transverse and longitudinal relaxation, and precession about the z axis, and is given by the following product:

$$R(n, \phi, \psi) = \begin{bmatrix} \cos(\psi + n\phi) & \sin(\psi + n\phi) & 0 \\ -\sin(\psi + n\phi) & \cos(\psi + n\phi) & 0 \\ 0 & 0 & 1 \end{bmatrix} \times \begin{bmatrix} E_2 & 0 & 0 \\ 0 & E_2 & 0 \\ 0 & 0 & E_1 \end{bmatrix} \begin{bmatrix} 1 & 0 & 0 \\ 0 & \cos \alpha & \sin \alpha \\ 0 & -\sin \alpha & \cos \alpha \end{bmatrix}. \quad (6)$$

\mathbf{M}_{eq} in Eq. (5) denotes the thermal equilibrium magnetization represented by a unit vector along the z axis.

If an initial condition for $n=0$ represented by a vector $(\mathbf{M}^-)_0$ is specified, the three-dimensional nonautonomous map represented by Eq. (5) can be iterated in order to examine the onset of a steady state. It is convenient, but not essential, to assume that the initial vector coincides with the vector $(\mathbf{M}^-)_0 = (\mathbf{M}^-)_s$ whose components $(M_\mu^-)_s$ ($\mu = x, y, z$) are the steady-state values corresponding to $v=0$ [Eqs. (1)–(4)]. Self-consistency then requires that the condition $\phi=0$ in $R(n, 0, \psi)$ of Eq. (5) should yield an output vector that is identical to this initial vector $(\mathbf{M}^-)_s$.

The matrix iteration algorithm of Eq. (5) did not demand, in general, excessively long computing time and the correctness of its results could be checked against the velocity dependence of the echo amplitude in conventional SSFP reported earlier [18]. Although some dynamical aspects of Eq. (5) in the parameter space spanned by $\phi = \gamma G v T_p^2$, T_2/T_p , and T_1/T_p are interesting from a more general point of view, we here focus on a limited range of values relevant to the present application. Numerical computations show that, as n increases beyond $5T_1/T_p$, the components $(M_\mu^-)_n$ ($\mu = x, y, z$) reach an effective steady state for this limited region of parameter space.

In this steady state, $(M_\mu^-)_n$ become periodic functions of n oscillating with period $\Delta n = 2\pi/\phi$, with phase shift governed by the offset angle ψ and amplitude controlled by ϕ . Moreover, the role of ψ in conventional applications of SSFP, for example, magnetic resonance imaging in the presence of flow, is quite different from that in the CWFP regime. In the former case, a wide dispersion $\Delta\psi$ prevails; consequently $(M_x^-)_n$ and $(M_y^-)_n$ for $n > 5T_1/T_p$ must be averaged over $0 < \psi < 2\pi$ with a uniform distribution [18]. The resulting average values $\langle M_\mu^- \rangle_\psi$ are found to be no longer oscillating and therefore independent of n as long as $n > 5T_1/T_p$. As a check, the average transverse magnetization, which determines the flow sensitivity in the SSFP regime, was calculated and compared with earlier results [18]. The agreement for various values of the parameters T_1/T_p , T_2/T_p , and α was found to be excellent.

We next focus on the flow sensitivity in the CWFP regime and its peculiar features. One first notices that, since the magnetic field gradient G as well as T_p are much smaller

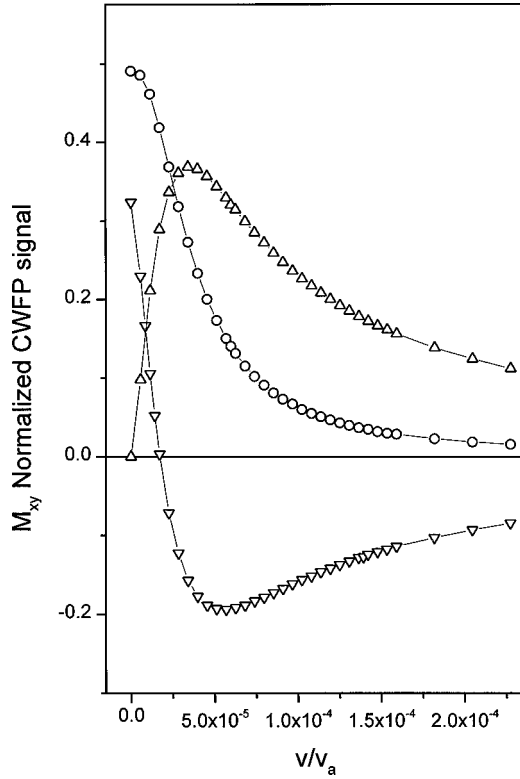


FIG. 1. Calculated CWFP normalized transverse magnetization for plug flow with $\lambda/l \approx 30$, $T_1/T_p = 9.5 \times 10^3$, $T_2/T_p = 9.2 \times 10^3$, flip angle $\alpha = \pi/2$, and various offset angles. $\psi = (\text{O}) (2n+1)\pi$, $(\Delta) 2n\pi$, and $(\nabla) (2n+1/4)\pi$ for $\mathbf{G} \cdot \mathbf{v} > 0$ or $(2n+7/4)\pi$ for $\mathbf{G} \cdot \mathbf{v} < 0$ ($n=0,1,2,3, \dots$). The abscissa represents the fluid velocity relative to the aliasing velocity.

than in conventional SSFP, the wavelength $\lambda = 2\pi/\gamma GT_p$ [18,19] is large compared with the length of the coil l and a spatially uniform magnetization is expected. Consider now an annular ring of fluid, moving with velocity v , just about to enter the coil region where the gradient is applied. The phase of this element of fluid must be $\psi + 2\pi m$ where m is an integer. At the same time, a similar element is leaving the coil after experiencing $l/v T_p$ pulses and therefore with an additional phase $(l/v T_p)\phi = l\gamma GT_p = (2\pi l)/\lambda$. The steady-state signal can be obtained by adding the contributions of all these fluid elements. This requires that for a given offset angle ψ and a given value of $\phi = \gamma v GT_p^2$ we must add the contributions of components $(M_{\mu}^-)_n$ of Eq. (5) with values n such that $(2\pi m/\phi) + (2\pi l)/\lambda > n > 2\pi m/\phi$. Moreover, for $l \ll \lambda$, the dominant contribution comes from the terms $(M_{\mu}^-)_n$ with $n \approx 2\pi m/\phi$, where the integer m must be sufficiently large to satisfy the condition $2\pi m/\phi > 5T_1/T_p$ necessary to achieve a steady state in Eq. (5).

III. EXPERIMENTAL RESULTS AND DISCUSSION

Experiments were performed in a home-built NMR apparatus described earlier [21]. A 1770 G bench-type permanent magnet was shimmed for maximum homogeneity in such a way that the residual gradient was small. A flow of deionized water ($T_1 = 2.85$ sec, $T_2 = 2.76$ sec) varying from zero to ap-

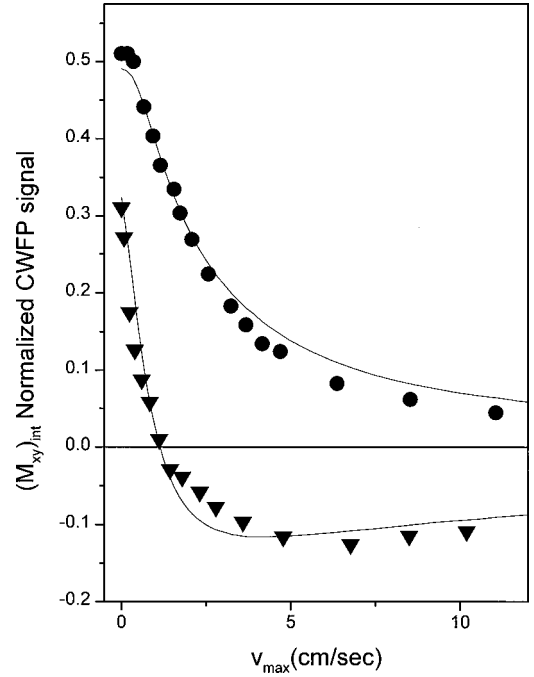


FIG. 2. Measured and calculated phase detected CWFP signals for a laminar flow of water in a pipe of radius $a = 0.4$ cm. The normalized signals are plotted as a function of the maximum velocity of the parabolic profile. The flip angle was $\alpha = \pi/2$ with $T_1 = 2.85$ sec, $T_2 = 2.76$ sec, $T_2^* = 20$ msec, and $T_p = 0.3$ msec. Two offset angles were employed. $\psi = (\bullet) 5\pi$ and $(\nabla) 23\pi/4$. Theoretical CWFP signals, shown as full lines, were calculated for $\psi = 5\pi$ and $23\pi/4$ ($\mathbf{G} \cdot \mathbf{v} < 0$) assuming a value $G = 0.097$ G/cm.

proximately 5 ml/sec was employed. The frequency offset from resonance ω_0 was adjusted so that the phase angle $\psi = \omega_0 T_p$ could attain any value in the range $4\pi < \psi < 6\pi$. Water solutions containing paramagnetic ions with various relaxation rates were also employed to corroborate the predicted dependence upon the relaxation parameters. In order to compare the results of Sec. II with our measurements, it was first necessary to integrate the velocity dependence of the magnetization components obtained from Eq. (5) over a uniform velocity distribution in the range $0 < v < v_{\max}$. The maximum velocity at the center of the parabolic radial profile of Poiseuille's law is given by $v_{\max} = 2Q/\pi a^2$, where Q denotes the measured volume flow (ml/sec) in a laminar regime and $a = 0.4$ cm is the internal radius of the cylindrical pipe.

Figure 1 illustrates the pronounced dependence of flow sensitivity upon frequency offset from resonance for CWFP conditions. The calculated normalized transverse magnetization (M_{xy}) for three values of the offset angle ψ is shown as a function of v/v_a for plug flow. Here $v_a = 2\pi/\gamma GT_p^2$ denotes the aliasing velocity [18,19] and the condition $l \ll \lambda$ has been assumed. A flip angle $\alpha = \pi/2$ and ratios $T_1/T_p = 9.5 \times 10^3$, $T_2/T_p = 9.2 \times 10^3$ appropriate for deionized water with $T_p = 0.3$ m sec have been used.

Figure 2 shows measured CWFP signals, also normalized with respect to the thermal equilibrium value, as a function of v_{\max} , the maximum velocity of the parabolic profile. Also shown are calculated values of $(M_{xy})_{\text{int}}$ obtained by an inte-

gration of the magnetization components used in Fig. 1. For the special offset angle $\psi = 23\pi/4 (\mathbf{G} \cdot \mathbf{v} < 0)$, $(M_{xy}^-)_{\text{int}}$ exhibits a node for $v_{\text{max}} = 1.1$ cm/sec, corresponding to a flow $Q_0 = 0.27$ ml/sec. For flow values larger than Q_0 , the phase detected CWFP signal actually changes sign as predicted theoretically.

In striking contrast with conventional SSFP, the flow sensitivity can be changed dramatically by slight changes in the frequency offset from resonance, as shown in Fig. 1. Even if the condition $T_p \ll T_2^*$ were only approximately satisfied and a partial integration over ψ values were necessary, these effects would not be completely masked. Furthermore, flow sensitivity is also expected, in general, to be different for $\mathbf{G} \cdot \mathbf{v} > 0$, corresponding to a magnetic field that increases along the direction of velocity, than for $\mathbf{G} \cdot \mathbf{v} < 0$. As can be inferred from Eq. (6), a change of sign in ϕ leaves the transverse magnetization invariant only if ψ , adjusted in practice in the range $4\pi < \psi < 6\pi$, is changed to $10\pi - \psi$. Thus, except for $\psi = 4\pi$, 5π , and 6π , substantial changes may occur when the direction of flow is inverted, as was observed experimentally.

We conclude that in the CWFP regime unusual flow ef-

fects are present. Even very small magnetic field gradients may cause a pronounced and peculiar flow sensitivity. In addition to the parameters that prevail in standard SSFP, the frequency offset from resonance and the direction of flow relative to the gradient play a dominant role in CWFP. Tailored flow sensitivity can be achieved by appropriate tuning of the frequency offset and might find useful applications in fine flow monitoring and control. Unlike in standard SSFP, the velocity dependence of the signal can be made to decay monotonically, to display a maximum for a certain velocity, or to have a null value. This signal null, which is followed by a phase inversion of 180° , is a distinctive flow signature of the CWFP regime.

ACKNOWLEDGMENTS

We thank Fundação de Amparo à Pesquisa e Desenvolvimento do Estado de São Paulo, Conselho Nacional de Desenvolvimento Científico e Tecnológico, Coordenadoria para Aperfeiçoamento de Pessoal de Ensino Superior, and Financiadora de Estudos e Projetos (Brazilian agencies) for support.

-
- [1] Ken J. Packer, in *Encyclopedia of Nuclear Magnetic Resonance*, edited by D. M. Grant and R. K. Harris (Wiley, New York, 1995).
 - [2] William S. Price, *Concepts Magn. Reson.* **10**, 197 (1998).
 - [3] P. T. Callaghan, A. Coy, T. P. J. Halpin, D. MacGowan, K. J. Packer, and F. O. Zelaya, *J. Chem. Phys.* **97**, 651 (1992).
 - [4] P. T. Callaghan and A. Coy, *Phys. Rev. Lett.* **68**, 3176 (1992).
 - [5] P. P. Mitra, P. N. Sen, L. M. Schwartz, and P. Le Doussat, *Phys. Rev. Lett.* **68**, 3555 (1992).
 - [6] P. P. Mitra, L. L. Latour, R. L. Kleinberg, and C. H. Sotak, *J. Magn. Reson A* **114**, 47 (1995).
 - [7] A. N. Garroway, *J. Phys. D* **7**, L159 (1974).
 - [8] R. J. Gummerson, C. Hall, W. D. Hoff, R. Hawkes, G. N. Holland, and W. S. Moore, *Nature (London)* **281**, 56 (1979).
 - [9] S. Blackband and P. Mansfield, *J. Phys. C* **19**, L49 (1986).
 - [10] P. Mansfield, R. Bowtell, and S. Blackband, *J. Magn. Reson.* **99**, 507 (1992).
 - [11] W. Schrader and J. B. Litchfield, *Drying Technol.* **10**, 295 (1992).
 - [12] P. L. de Souza, M. Engelsberg, and F. G. Brady Moreira, *Phys. Rev. E* **60**, R1174 (1999).
 - [13] H. Y. Carr, *Phys. Rev.* **112**, 1693 (1958).
 - [14] R. R. Ernst and W. Anderson, *Rev. Sci. Instrum.* **37**, 93 (1966).
 - [15] R. Freeman and H. D. W. Hill, *J. Magn. Reson.* **4**, 366 (1971).
 - [16] W. S. Hinshaw, *J. Appl. Phys.* **47**, 3709 (1976).
 - [17] S. Patz and R. C. Hawkes, *Magn. Reson. Med.* **3**, 140 (1985).
 - [18] Hakon Gudbjartsson and Samuel Patz, *Magn. Reson. Med.* **34**, 567 (1995).
 - [19] M. Tyszka, R. C. Hawkes, and L. D. Hall, *J. Magn. Reson B* **101**, 158 (1993).
 - [20] R. Buxton, *Magn. Reson. Med.* **29**, 235 (1993).
 - [21] Rodrigo B. V. Azeredo, Luiz A. Colnago, and M. Engelsberg, *Anal. Chem.* **72**, 2401 (2000).